European Journal of Neuroscience, Vol. 25, pp. 785–794, 2007 doi:10.1111/j.1460-9568.2007.05308.x

Stochastic description of complex and simple spike firing in cerebellar Purkinje cells

Soon-Lim Shin,[1] Stefan Rotter,[2,3] Ad Aertsen[2,4] and Erik De Schutter[1]
[1]Theoretical Neurobiology, University of Antwerp, Universiteitsplein 1, B2610, Antwerp, Belgium
[2]Bernstein Center for Computational Neuroscience, Freiburg, Germany
[3]Theory and Data Analysis, Institute for Frontier Areas of Psychology and Mental Health, Freiburg, Germany
[4]Neurobiology and Biophysics, Institute of Biology III, Albert-Ludwigs-University, Freiburg, Germany

Keywords: anaesthetized rat, coefficient of variation, inferior olive, order, rate

Abstract

Cerebellar Purkinje cells generate two distinct types of spikes, complex and simple spikes, both of which have conventionally been considered to be highly irregular, suggestive of certain types of stochastic processes as underlying mechanisms. Interestingly, however, the interspike interval structures of complex spikes have not been carefully studied so far. We showed in a previous study that simple spike trains are actually composed of regular patterns and single interspike intervals, a mixture that could not be explained by a simple rate-modulated Poisson process. In the present study, we systematically investigated the interspike interval structures of separated complex and simple spike trains recorded in anaesthetized rats, and derived an appropriate stochastic model. We found that: (i) complex spike trains do not exhibit any serial correlations, so they can effectively be generated by a renewal process, (ii) the distribution of intervals between complex spikes exhibits two narrow bands, possibly caused by two oscillatory bands (0.5–1 and 4–8 Hz) in the input to Purkinje cells and (iii) the regularity of regular patterns and single interspike intervals in simple spike trains can be represented by gamma processes of orders, which themselves are drawn from gamma distributions, suggesting that multiple sources modulate the regularity of simple spike trains.

Introduction

Purkinje cells (PCs), the only output neurones of the cerebellar cortex, generate two distinct types of spikes, complex spikes (CSs) and simple spikes (SSs). In anaesthetized rats CSs occur at very low frequencies (mean spontaneous firing rate, 1.3 Hz; range, 0.2–4.7 Hz), whereas SSs discharge at high firing rates (mean spontaneous firing rate, 27.9 Hz; range, 4.0–81.4 Hz) (Bower & Woolston, 1983; Vos *et al.*, 1999; Brown & Bower, 2001). CSs are caused by activation of a climbing fibre, whereas SSs are assumed to be disynaptically triggered by mossy fibres via parallel fibres (PFs), which are the axons of granule cells in the cerebellar cortex. It is likely that two anatomically separate afferent systems will transfer information in parallel. Although SS firing is known to be strongly influenced by CSs, which usually cause a pause in SS firing (Ebner & Bloedel, 1981; Sato *et al.*, 1992), CSs are generally assumed to occur independently of SSs.

Both CS and SS trains have been described as highly irregular, expressed by a high coefficient of variation (CV) (Vos *et al.*, 1999; Goossens *et al.*, 2001), but the underlying structure of the irregular spike trains is poorly understood. If consecutive interspike intervals (ISIs) are independent of each other, the theory of renewal processes can be used to investigate the underlying processes (Dayan & Abbott, 2001). Because of the independence of ISIs, spike trains generated by a renewal process are statistically fully specified by their ISI distribution function (Tuckwell, 1988). In other words, if spikes are generated by a renewal process, the ISI distribution will give the underlying process. For instance, if the ISI probability density function can be fitted by an exponentially decaying function, the process would be a Poisson process that is defined by a single parameter, the firing rate. If, more generally, a gamma distribution provides the best fit, the underlying process is called a gamma process, defined by two parameters, the so-called order and mean firing rate.

In a previous study we showed that SSs recorded in anaesthetized and awake rodents are not simple renewal processes, such as a Poisson process, because of the unexpectedly frequent occurrence of highly regular spike patterns (Shin *et al.*, 2004; Shin & De Schutter, 2006). This, however, does not exclude that SS trains are composed of a mixture of multiple different renewal processes. Likewise, it is not at all clear yet whether CSs can be described by a renewal process. In the present study we tried to fit spontaneous CS and SS activity recorded in anaesthetized rats with mixtures of different renewal processes. Although many renewal processes have been studied (Tuckwell, 1988), we restricted ourselves here to one of the best-known types, the gamma processes. Gamma processes are quite general, encompassing the Poisson process as a special case (order 1), and are relatively simple to handle. Moreover, the parameters of a gamma process can be easily linked to physiological parameters, regularity (order) and mean firing rate.

Materials and methods

Recordings

Sprague-Dawley rats ($n = 23$, 300–500 g, Iffa Credo, Brussels, Belgium) were anaesthetized with a mixture of ketamine HCl

Correspondence: Professor E. De Schutter, as above.
E-mail: erik@tnb.ua.ac.be

Received 11 July 2006, revised 24 October 2006, accepted 19 November 2006

(75 mg/kg; Ketalar, Parke-Davis, Warner Lambert Manufacturing, Dublin, Ireland) and xylazine HCl (3.9 mg/kg; Rompun, Bayer, Leverkusen, Germany) in normal saline (0.9% NaCl, Baxter, Lessine, Belgium) by intraperitoneal injection. A craniotomy exposing crus I and II of the left cerebellar hemisphere was performed (Vos *et al.*, 1999). Supplemental doses of the anaesthetic (one-third of the initial dose) were given intramuscularly to maintain deep anaesthesia as demonstrated by the lack of a pinch withdrawal reflex and/or lack of whisking. Forty single-unit recordings of spontaneous activity were made in the cerebellar cortex with tungsten microelectrodes (impedance ~10 MΩ, FHC, Bowdoinham, ME, USA). Signals were filtered and amplified (bandpass, 0.5–9 kHz; gain, 5000–10 000) using a multichannel neuronal acquisition processor (Plexon Inc., Austin, TX, USA). All experimental methods were approved by the ethical commission of the University of Antwerp and conformed to European Union guidelines.

Data analysis

The CSs and SSs were further sorted using an off-line sorter (Plexon Inc.). The mean firing rates of CS and SS were 0.74 ± 0.05 and 40.7 ± 3.6 Hz, respectively. All analyses and simulations were performed off-line using MATLAB (MathWorks, Natick, MA, USA) and EXCEL (Microsoft, Redmond, WA, USA). Joint interval histograms of CSs (presented in Fig. 2) were made with variable bin sizes (number of bins = 5 or 6), ensuring that each bin contained at least 10 intervals and not more than one-quarter of all intervals. Specifically, the upper bound of the first bin was adjusted between 150 and 400 ms, and those of the second, third and fourth bins were chosen between 600 and 1000 ms, 1500 or 2000 ms, and between 2500 and 3500 ms, respectively. The fifth bin was the last bin containing the maximum ISI if the number of intervals was not over one-quarter of all intervals, otherwise there was one more bin up to 5000 ms.

The averaged irregularity of spike trains was measured by the CV (SD of ISIs/mean of ISIs) and the short range irregularity was measured by $CV_2 = 2|ISI_i - ISI_{i+1}|/(ISI_i + ISI_{i+1})$ (Holt *et al.*, 1996). Throughout this study, the mean of the CV_2 values (mCV_2), computed over the complete spike train, was used to represent the averaged short range variability. We used the CV_2 method to classify all ISIs in an SS train as belonging to either regular patterns or singles (Shin *et al.*, 2004). A regular pattern was defined as consecutive ISIs where all CV_2 values calculated with those ISIs were smaller than or equal to 0.24. The start of a regular pattern can be defined at a spike where CV_2 calculated with two ISIs surrounding the spike was larger than 0.24 followed by a spike with a CV_2 value lower than 0.24. All ISIs not belonging to regular patterns were called singles, which was 43% of all spikes (see Shin *et al.*, 2004 for details).

Data are represented as mean ± SEM unless otherwise stated. All *P*-values refer to Student's *t*-test unless otherwise specified.

Stochastic modelling

Both the estimation of parameters (gamma order and rate) and generation of random intervals were performed using MATLAB. The order and rate parameters for the best-fitting gamma distribution were obtained using the built-in MATLAB function gamfit(). In all simulations, a refractory period equal to the minimum ISI of corresponding spike trains was explicitly implemented because intrinsically generated refractory periods by gamma processes (especially when the order was less than 10) were often shorter than the actual minimum ISIs measured.

As a control, we first determined how many ISIs were required to obtain a proper estimate of the order parameters. We estimated the orders for a certain number of ISI (5, 10, 20, 50, 100, 200, 500 and 1000) taken from known gamma distributions with a fixed order (1, 2, 5, 10, 20, 50 and 100). We then calculated the ratio of the estimated order, determined as the average over 10 simulations, to the theoretically expected order for firing rates of 20 and 50 Hz (Fig. 1A). In both cases, the ratio was significantly greater than 1 ($P < 0.001$, χ^2 test) when the estimate was made with only five or 10 ISIs. We checked for any systematic relation between this ratio and the computed order when only five ISIs were used. We did not find any relation athough there was clearly more fluctuation when the firing rate was lower (Fig. 1B) (see also Nawrot *et al.*, 2003).

The same number of simulated as recorded CS trains ($n = 39$) was generated using the stochastic model constructed in this study, where parameters for each train were estimated from each experimental recording. The number of ISIs in each simulated CS spike train was the same as that in the corresponding recorded CS train. Forty simulated CS trains were generated using the MATLAB toolbox 'Filter Design' based on an explanatory model described in the Results (simulation duration, 200 s; sampling frequency, 1 ms). In these simulations, simulated CS trains were accepted only if their mean firing rate fell within the range of the experimental data (0.19–1.60 Hz).

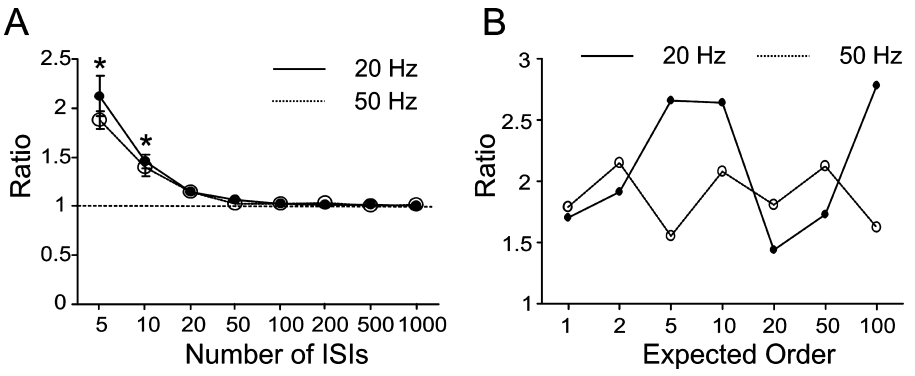

FIG. 1. Required number of interspike intervals (ISIs) to estimate a correct order parameter. (A) The averaged ratio of estimated order to expected order (1, 2, 5, 10, 20, 50 or 100) for different numbers of ISIs used in the estimate (*x*-axis) from 10 trials. The order was significantly overestimated when the number of ISIs was 5 or 10 (*$P < 0.001$, χ^2 test) for rates of both 20 (●) and 50 (○) Hz. The dotted line marks a quotient of 1 obtained for correct estimates. (B) Fluctuating estimated order for 20- or 50-Hz frequency when the number of ISIs was 5.

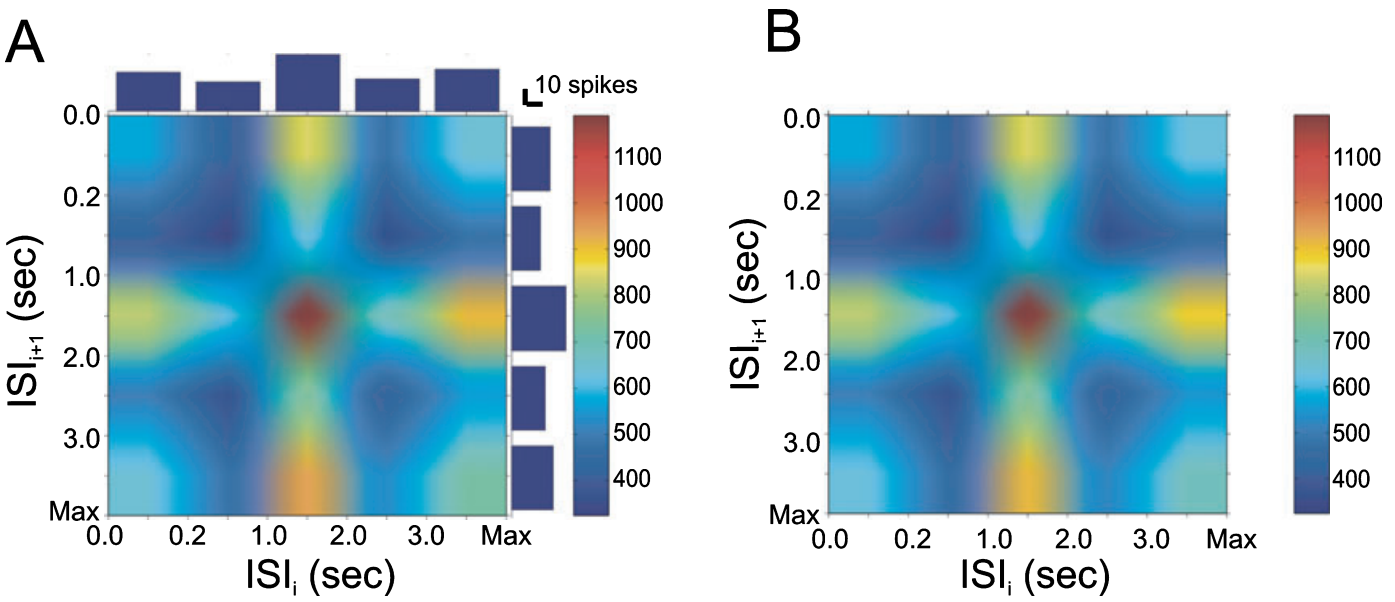

FIG. 2. Renewal complex spike (CS) spiking. (A) Joint interval histogram of consecutive interspike intervals (ISIs) in a representative CS train. Individual ISI distributions are shown on the top (ISI_i) and on the right side (ISI_{i+1}). (B) Joint interval histogram obtained by multiplying two individual ISI distributions shown in A. Both joint interval histograms have variable bin size containing at least 10 ISIs (see Materials and methods).

Results

Characteristics of complex spike spiking patterns

We first established whether spontaneous CS trains observed in anaesthetized rats can be considered as realizations of a renewal process. This requires that the consecutive intervals ISI_i and ISI_{i+1} are statistically independent. If this is the case, a joint interval histogram of consecutive ISIs will be the same as that obtained by cross-multiplying two corresponding marginal histograms because the marginal histogram (i.e. the conventional ISI histogram) does not contain any temporal order information. To test this, we compared two joint histograms, one the actual joint interval histogram counting the number of successive interval pairs in each bin (Fig. 2A) and the other obtained by cross-multiplying the ISI distribution [shown on the top (ISI_i) and right side (ISI_{i+1}) of Fig. 2A] with itself (Fig. 2B). These two histograms were not significantly different ($P > 0.99$, χ^2 test), indicating that successive intervals were indeed independent and hence that CSs were generated by a renewal process.

However, CS trains could not be described by a simple gamma process. In fact, most CS trains showed significantly higher mCV_2 values (1.00 ± 0.02, range 0.71–1.30) than CV (0.89 ± 0.02, range 0.76–1.22, $P < 10^{-6}$), implying that CS ISIs were more variable over short time ranges than for long-term averages. This is suggestive of a sudden switch of two very different distributions of ISIs. This was confirmed by inspection of the ISI distribution of CS trains, which clearly revealed a mixture of at least two ISI distributions, one with a narrow peak at around 100 ms and the other with a very broad peak between 1 and 2 s (Fig. 3). To separate these two distributions, we set a threshold at 400 ms, chosen by visual inspection. On average, 25.1 ± 1.7% of ISIs were shorter than or equal to 400 ms. The corresponding frequency distributions were unexpectedly narrow, from 4 to 8 Hz (5.70 ± 0.13 Hz, Fig. 4, dotted line with open circles) for the group with short ISIs and from 0 to 1 Hz (0.55 ± 0.03 Hz, Fig. 4, solid line with filled circles) for the other group. Note that no frequencies were observed around 2.5 Hz, the chosen threshold value. This confirms that there were indeed two clearly separated groups of

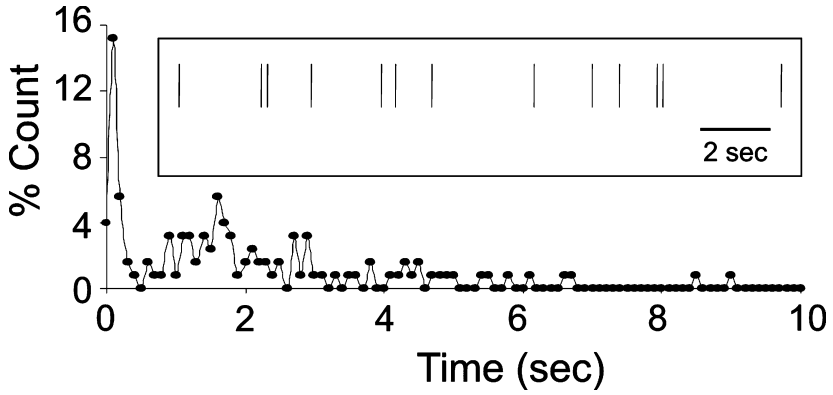

FIG. 3. Firing pattern of complex spike (CS). ISI histogram of a representative CS train (number of spikes, 126; recording duration, 259.9 s). Inset: raster plot of CS firing for 20 s.

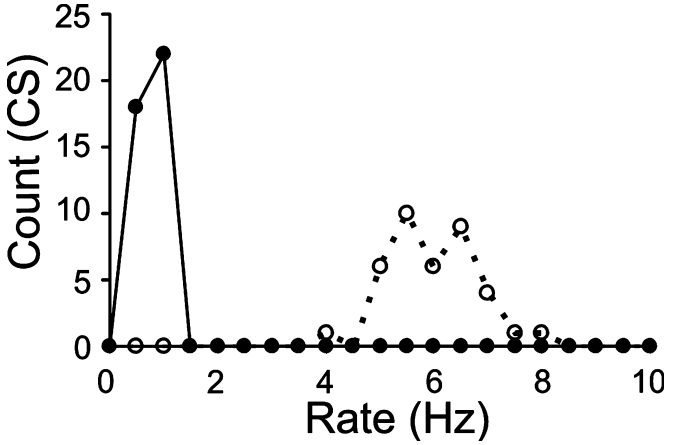

FIG. 4. Rate distribution of complex spike (CS). Rate histogram for two groups of interspike intervals (ISIs) estimated in each CS train, computed as the inverse of the means for each group, obtained from all 40 CS trains. Dotted line, ISIs shorter than or equal to 400 ms; solid line, ISIs longer than 400 ms. Bin = 0.5 Hz.

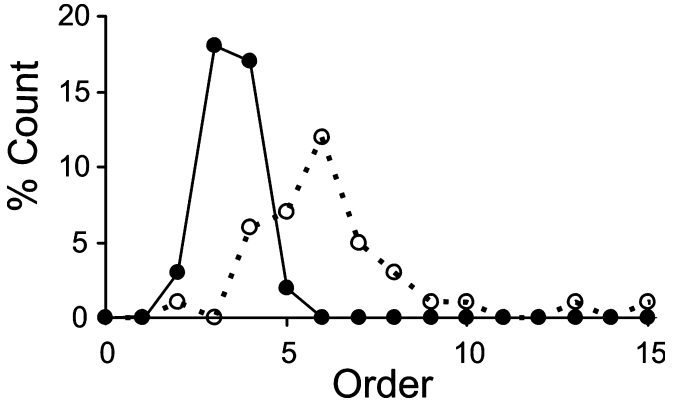

FIG. 5. Distribution of order parameters. Distributions of orders estimated from the distribution of interspike intervals shorter than or equal to 400 ms (dashed line with ○) and those longer than 400 ms (solid line with ●).

ISIs in each CS train, one longer than or equal to 1 s and the other shorter than 250 ms.

In the next step, we tested whether CS trains could be fitted by a random mixture of two gamma processes, separately obtained from groups of ISIs shorter or longer than 400 ms. Both order and rate parameters were obtained for each group separately from the best-fitting gamma distribution. Shorter ISIs exhibited higher orders (5.8 ± 0.4) than the longer ISIs (3.0 ± 0.1, $P < 10^{-6}$, Fig. 5). The rate parameters were equal to the mean values of the ISIs divided by their estimated orders. From the two sets of estimated parameters from each CS train, i.e. two order parameters and the associated two rate parameters, two groups of random ISIs were generated and then randomly mixed to obtain a final simulated CS train by permuting all random ISIs that were a sequence of two groups of randomly generated ISIs. We found that these simulated CS trains were indeed very similar to the real ones (Fig. 6A, gray), with a similar ISI histogram (Fig. 6B, gray, correlation coefficient = 0.88 for the example; on average correlation coefficient = 0.80 ± 0.03) and similar statistical properties, such as CV, mCV_2, mean and median of ISI (Fig. 6, inset, open bar, $P > 0.4$).

A possible neuronal mechanism to generate the two groups of ISIs is depicted in Fig. 7. Here, we assumed that the membrane potential of the inferior olivary neurones, the only source of climbing fibre activity, fluctuates with a mixture of two noisy frequency bands. These two frequency bands were generated by filtering white noise using two equiripple band-pass filters, ranging either from 4 to 8 Hz (Fig. 7A, dotted line) or from 0 to 1 Hz (Fig. 7A, dashed line). The resulting combined oscillatory process depends on the relative gains (amplitudes) of the two component bands. Defining the amplitude of the fast oscillation as α, that of the slow oscillation is $(1 - \alpha)$. An additional important parameter necessary to generate spikes from the fluctuating membrane potential is the spiking threshold. Thus, in addition to the frequency bands used, this explanatory model requires two parameters, the relative amplitude α and the spiking threshold. To tune these parameters to fit the neuronal data, we calculated the mean firing rate, CV and mCV_2 for different α values (from 0 to 1 with intervals of 0.1) at two different thresholds (0.2 and 0.3, Fig. 7B–D). By comparing the mean ± SD, we found a unique set of parameters that, for the entire set of CS recording data ($N = 39$), produced simulated CS spike trains in the physiological range ($\alpha = 0.2$ and threshold = 0.3, Fig. 7B–D, open arrows). Figure 8A shows solid line an example with the spikes generated from the summation (solid line) of two individual oscillations with gains of 0.2 (fast oscillation, dotted line) and 0.8 (slow oscillation, dashed line) at the threshold of 0.3 (thin solid line). The resulting simulated spike train (Fig. 8B, inset) revealed very similar firing patterns and ISI histogram (Fig. 8B) as the real data (Fig. 6). The statistical properties (mean and median of ISI, CV and mCV_2) of the simulated spike trains ($N = 40$) were also similar ($P > 0.1$) (Fig. 8B, inset), suggesting that the precise temporal structure of the two different gamma processes may not be important at least for spontaneous CS trains.

Stochastic description of regular spike patterns and single intervals in simple spike trains

In a previous study, we reported that SS trains contain highly regular spike patterns (see Materials and methods for details), comprising series of 2–182 similar ISIs, which contain more than half of all SS ISIs (Shin *et al.*, 2004). The ISIs not belonging to regular patterns were called singles and represented mostly the high-end tail of the ISI distribution. We also showed that SSs are not generated by a simple renewal process, like a Poisson process. However, it remains possible that the ISIs in patterns are generated by a high-order gamma process that renders it regular, whereas singles are generated by another more irregular, i.e. lower order, gamma process.

To test this hypothesis, we searched for possible gamma order parameters for regular patterns and singles separately. We computed the orders of regular patterns. As we needed at least 20 ISIs to obtain the correct order estimate (see Materials and methods), we estimated orders only for patterns with more than 20 ISIs. This resulted in 1546 orders from 1.3 ± 0.6% of all regular patterns. Surprisingly, the distribution of orders (mean, 110.1 ± 1.7; median, 97.5; Fig. 9A, black) was itself a gamma distribution, with order parameter of 2.8 and a rate parameter of 39.5 (Fig. 9A, dashed line; $N = 1546$). The orders of regular patterns were not related to their mean ISI (Fig. 9B). On average, more than 80% of pattern mean ISIs were shorter than 20 ms (Fig. 9C). As short patterns (less than 20 ISIs) are otherwise statistically indistinguishable from long patterns (Shin *et al.*, 2004), we assumed that short patterns are generated by a similar process to long patterns. Thus, we will later use the fit of Fig. 9A to generate all regular patterns, both short and long.

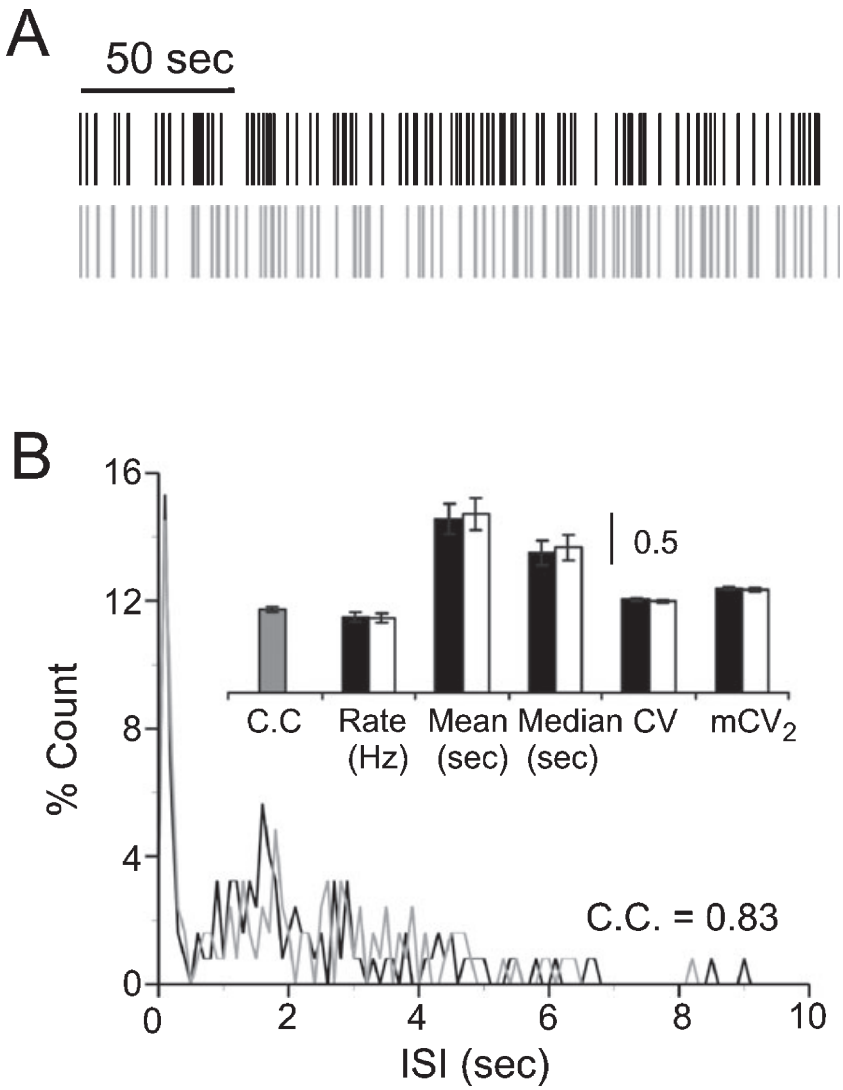

FIG. 6. Simulated complex spike (CS) train. (A) Raster plots of the same CS train as one demonstrated in Fig. 3 (black lines) and of the simulation of mixed two gamma processes (gray lines) for 200 s. The order parameter was 6.3 (2.6) and rate parameter was 6.4 (0.4) for interspike intervals (ISIs) shorter than or equal to 400 ms (or longer than 400 ms). (B) ISI histograms of the spike trains shown in A. Inset: mean correlation coefficients (CCs, gray filled bar), mean (s), median (s), coefficient of variation (CV) and mean of the CV_2 values (mCV_2) of ISIs were similar in actual (black filled bars) and simulated (open bars) CS trains ($P > 0.4$).

The interval distribution of single ISIs differed significantly from that of regular patterns ($P < 10^{-6}$, χ^2 test, Fig. 10A vs. Fig. 9C). Specifically, the singles comprised distinctly fewer short intervals. If all singles were generated by the same gamma process, the estimated order from the distribution of all singles should be equal to CV^{-2} (Gabbiani & Koch, 1998). We found, however, that the orders were significantly different from CV^{-2} ($P < 0.04$, Fig. 10B), indicating that singles are not caused by a single gamma process. This still leaves open the possibility that they were caused by a mixture of multiple processes. To estimate the orders of these presumed processes, we first took all singles from each SS train. For each of these we estimated the order for the first 20 singles, then moved to the next single and performed the next estimation, and repeated this procedure until the end of the singles, which is a similar procedure to estimating rates using sliding windows. After each estimation, we checked if the obtained order estimate was 1 or larger and that it was similar to CV^{-2} within a 20% error range. In total, 29.3% ($N = 5978$) of the orders thus estimated satisfied this criterion. The orders of the regular patterns also exhibited a gamma distribution (mean, 4.63 ± 0.03; median, 4.12) but with different parameters (order parameter 5.35 and rate parameter 0.87) (Fig. 10C, equal $N = 5978$; correlation coefficient = 0.98).

To test the feasibility of a statistical description of regular patterns and singles, we constructed a new, artificial spike train by replacing regular patterns and individual singles from a given recorded SS train with randomly generated regular patterns and singles using the above-described distributions (Figs 9A and 10C). A single parameter estimation was performed for all ISIs of each pattern and for each single. More specifically, ISIs of regular patterns (respectively, individual single ISIs) were created by randomly choosing an order from the distribution of Fig. 9A (respectively, Fig. 10C) and converting each pattern mean ISI (respectively, single ISI) to a rate parameter by dividing it by the chosen order. The randomly created spike trains showed firing patterns that were very similar to the original spike trains (Fig. 11A). On average, the simulated spike trains revealed very similar ISI distributions (Fig. 11B) and autocorrelograms (Fig. 11B, insets) with high correlation coefficients of 0.989 ± 0.002 and 0.969 ± 0.005, respectively. Statistical properties, such as the mean firing rate, mean, median, CV and mCV_2, were also

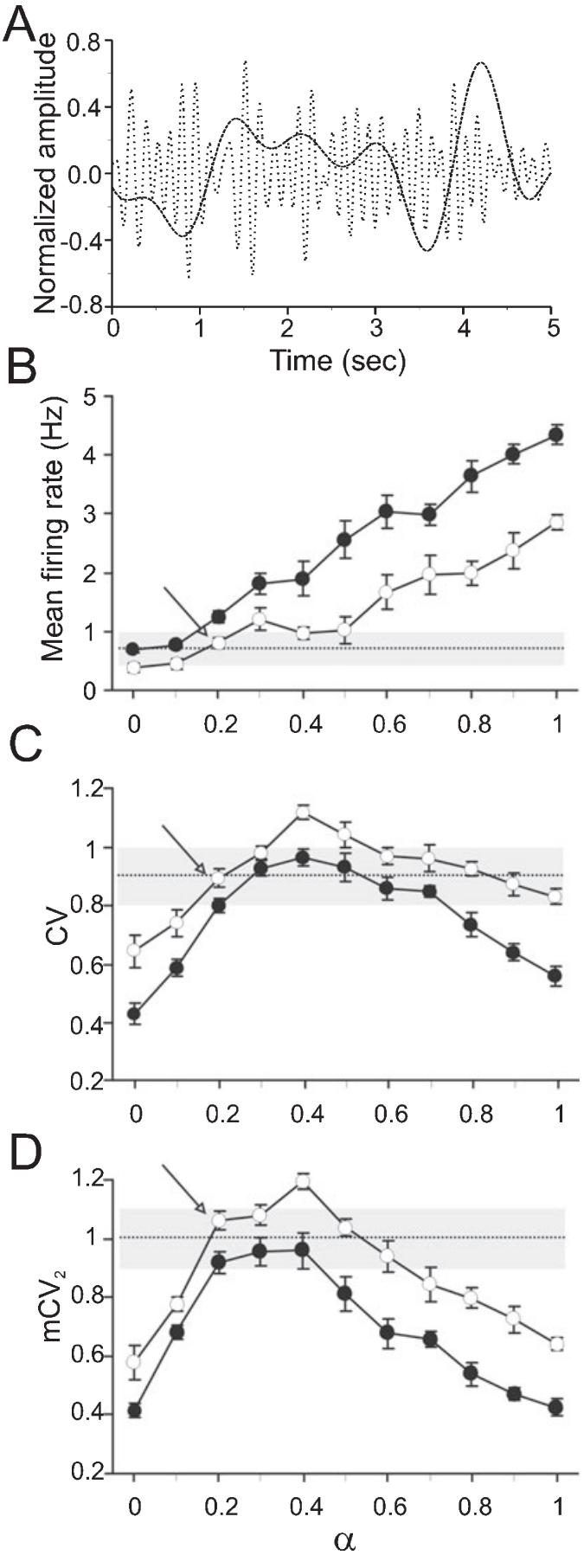

similar ($P > 0.5$, Fig. 11C). Only in cases with a slow modulation of firing rate in the recorded data, such as the 1- or 2-Hz oscillation in the right panel of Fig. 11B, was this oscillation not captured by the model that, by its stationary nature, only captured the average firing rate.

Unfortunately, this stochastic description of SS trains does not include any switching rule for the transitions between regular patterns and singles. As a first step in this direction we computed the switching probabilities for different processes. There are five possible transitions between two consecutive ISIs: from a pattern to the same pattern, from a pattern to a different pattern, from a pattern to a single, from a single to a pattern or from a single to another single. In our data sets, these transitions occurred with probabilities of 0.39 ± 0.03, 0.04 ± 0.00, 0.12 ± 0.00, 0.12 ± 0.00 or 0.33 ± 0.03, respectively, suggesting high chances that if an ISI belonged to a regular pattern (single), the next ISI would belong to the same regular pattern (respectively, single). In addition, on average 26.6 ± 1.3% of regular patterns were followed by a different regular pattern. However, these probabilities do not give any information on the change in rate accompanying a transition between regular patterns or between singles and regular patterns, which is essential to model the spike trains. There was a significant difference of median ISIs between regular patterns (12.9 ± 0.8 ms, Fig. 9C) and singles (17.6 ± 0.9 ms, Fig. 10A) ($P < 10^{-6}$; see also Shin *et al.*, 2004). There was also a significant difference between the mean ISIs of regular patterns switching to other patterns (12.5 ± 0.8 ms) and those switching to singles (13.0 ± 0.9, $P < 0.0005$) but this difference was too small to explain the threefold difference in transition probabilities.

Discussion

In this study, we have shown that spontaneous cerebellar PC CS and SS firings in anaesthetized rats can be described by a mixture of multiple gamma processes. CS spiking may be a random mixture of two gamma processes, which can be caused by two independent subthreshold oscillatory processes of the input system, the inferior olivary neurones. Subthreshold oscillations of membrane potential in inferior olivary neurones with a frequency between 4 and 10 Hz, and amplitudes varying between 3 and 10 mV have been reported in guinea pig inferior olivary neurones *in vitro* (Llinas & Yarom, 1986; Manor *et al.*, 1997; Yarom & Cohen, 2002). However, it is not yet clear whether the PC CS activity is oscillatory or not. For example, no oscillatory behaviour was reported in the PC CS activity recorded in awake monkeys (Keating & Thach, 1995), whereas rhythmic activity was found in PC CS trains recorded in awake rats (Lang *et al.*, 1999). Both studies were based on the autocorrelogram obtained from overall CSs. However, the absence of a significant serial correlation in the CS train (Fig. 2) suggests that the autocorrelogram may not be an optimal measurement to capture the fast switching oscillatory behaviour proposed here, which may have led to a misinterpretation regarding the CS firing patterns.

We showed that the short-range variability found in CS trains can be explained by a mixture of two different oscillatory processes with very

FIG. 7. Parameter search for an explanatory model to generate complex spike (CS). (A) Membrane potential, which is a combination of two normalized band-pass-filtered noises (dashed line, 0.5–1 Hz; dotted line, 4–8 Hz), generated by adding them with a variable multiplier (α for 4–8 Hz; 1 − α for 0.5–1 Hz). Mean firing rate (B), coefficient of variation (CV) (C) and mean of the CV_2 values (mCV_2) (D) of spikes that were generated by setting two different thresholds at 0.2 (black circles) or 0.3 (white circles) were calculated for different α (*x*-axes). Dashed lines, mean values of recorded CS trains; gray area, ± SDs of measurements. Open arrows show a set of parameter (α = 0.2, threshold = 0.3) in the physiological range.

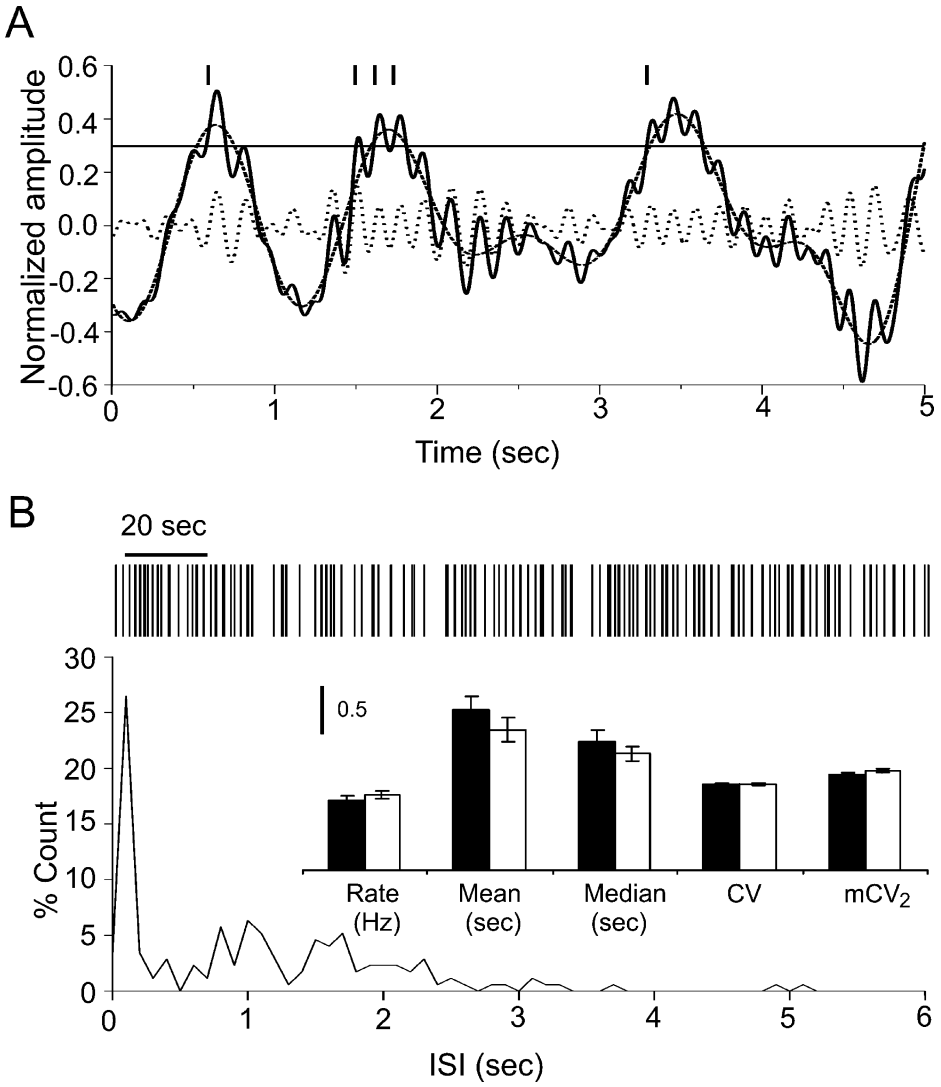

FIG. 8. Explanatory model for complex spike (CS) generation. (A) Expected CS (black vertical lines) by setting a threshold at 0.3 (thin solid) for the fluctuating membrane potential (thick solid), which is the sum of two band-pass-filtered noises (dashed line, 0.5–1 Hz; dotted line, 4–8 Hz), where $\alpha = 0.2$ and threshold $= 0.3$. (B) Raster plot for the overall simulated CS (top) and ISI histogram of simulated CS (duration 200 s). Inset: mean (s), median (s), coefficient of variation (CV) and mean of the CV_2 values (mCV_2) of interspike intervals (ISIs) were similar in actual (filled bars) and simulated (open bars) CS trains ($P > 0.1$).

different frequencies, one with a frequency range from 0.5 to 1 Hz and the other ranging from 4 to 8 Hz. In fact, such division of frequency bands is already suggested by the ISI distribution of CS trains showing two clearly separated distributions. Moreover, we found that, in order to obtain similar firing properties to those of CS trains recorded from anaesthetized rats, the amplitude of the low-frequency band should be some five times larger than that of the higher frequency band. This suggests that, in the anaesthetized *in-vivo* situation, an additional slow oscillatory process may modulate the faster oscillations observed in inferior olivary neurones *in vitro*.

Our results are limited to the spontaneous activities recorded in anaesthetized rats. In general, the CS mean firing rates reported in awake animals are higher than those in this study (Keating & Thach, 1995; Lang *et al.*, 1999). However, single trial traces of CS firing in awake monkeys show some shorter CS ISIs intermingled with longer ones (Keating & Thach, 1995). Thus, an interesting question is whether the higher mean firing rates of CS trains recorded in awake animals are caused by higher proportions of the high-frequency band and whether different behavioural tasks increase specific frequencies.

In contrast to CS firing, which was shown to be a renewal process, SS firing cannot be a simple renewal process as it contains regular patterns that imply strong serial correlations (Shin *et al.*, 2004). Thus, in the present study we focused on characterizing the stochastic properties of regular patterns and singles separately. The simplest scenario is that regular patterns are generated by gamma processes of higher orders and singles by lower order processes, more similar to Poisson processes. As expected, regular patterns were about 20 times more regular than singles. Moreover, orders estimated from both regular patterns and singles were not fixed but they showed a gamma distribution, suggesting that there are separate processes that independently regulate two distinct levels of regularity in SS firing. Note that we could obtain fairly good descriptions about regular patterns and singles from the order distributions obtained from only 1.3 and 29.3% of all patterns and singles, respectively. Unfortunately at present we cannot formulate a stochastic model that includes the transitions between regular patterns and singles.

The question then is how PCs can generate regular patterns and singles separately. One possible mechanism for regular patterns is that

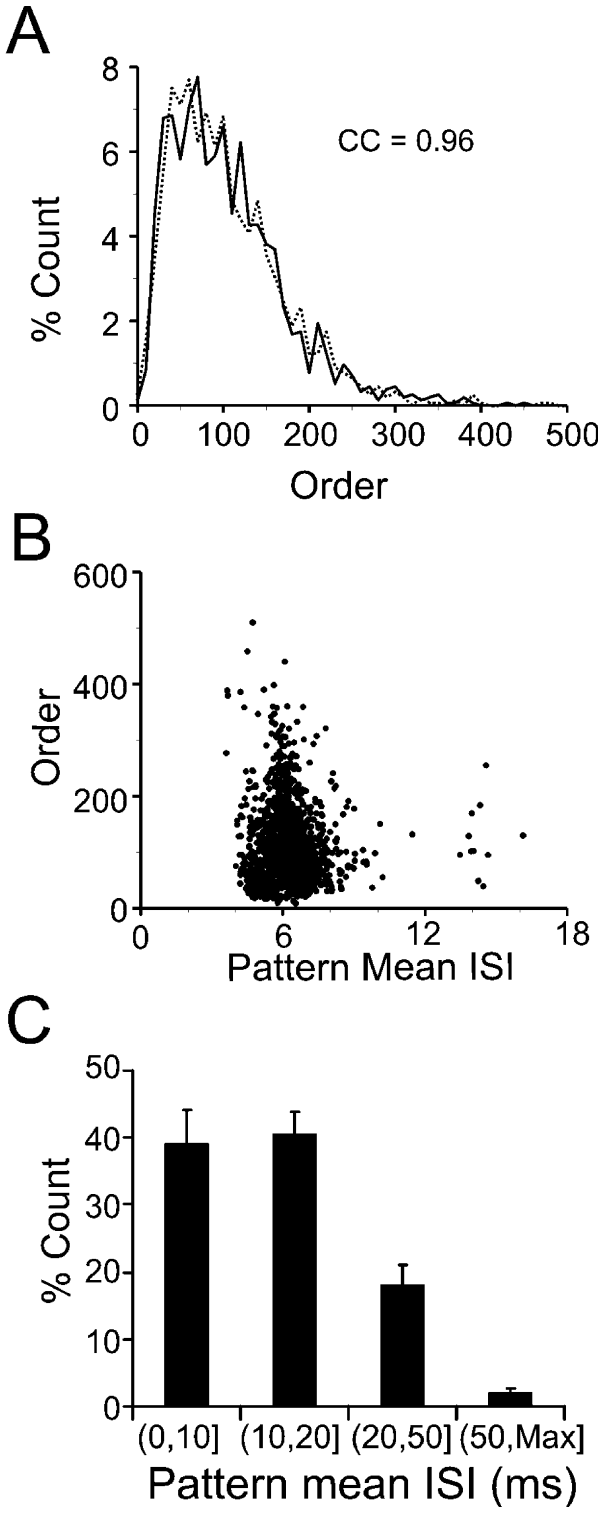

FIG. 9. Characteristics of regular patterns. (A) Distribution of orders estimated from patterns that contained 20 or more interspike intervals (ISIs) (solid line, bin = 10) of all simple spike (SS) trains was fitted [correlation coefficient (CC) = 0.97] with a gamma process whose order parameter was 2.8 and rate parameter was 39.5 (dotted line). (B) There was no relation between pattern mean ISI and their order. (C) Averaged distribution of pattern mean ISIs of regular patterns.

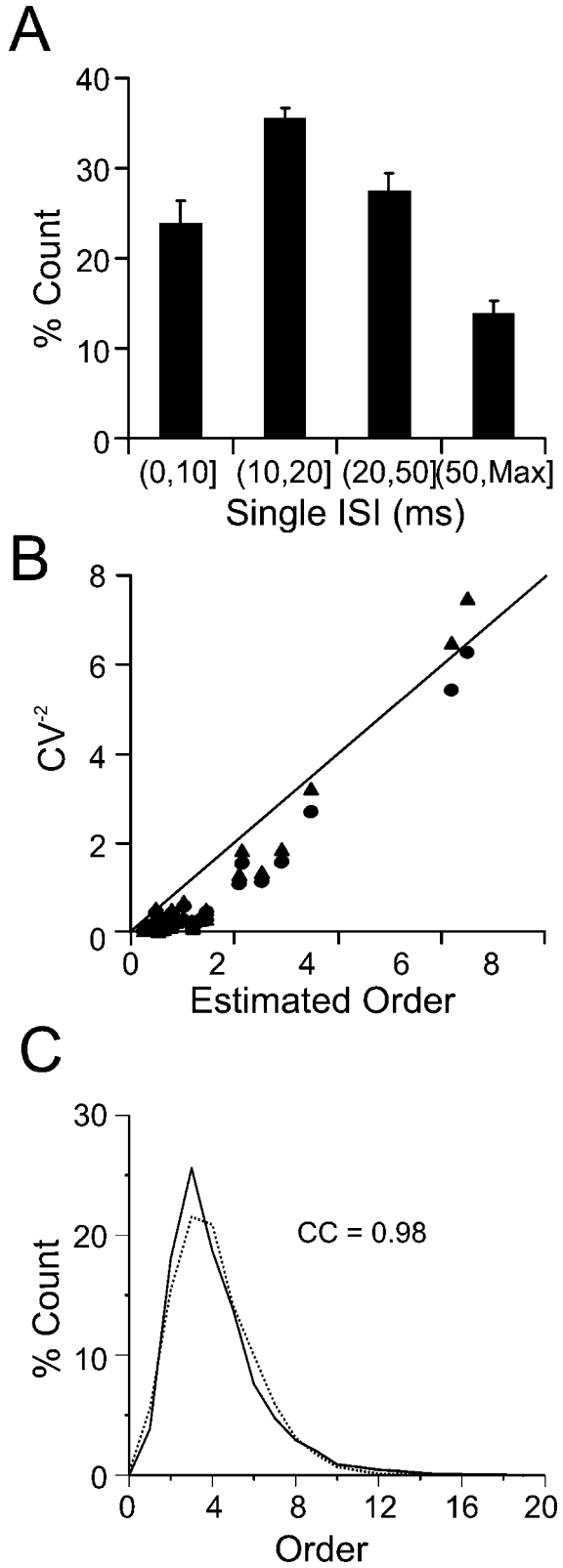

FIG. 10. Characteristics of singles. (A) solid line The averaged distribution of single interspike intervals (ISIs). (B) The estimated orders from all singles from each simple spike (SS) train were different from expected orders based on coefficient of variation CV^{-2} ($P < 0.04$, Student's *t*-test). (C) Distribution of correctly estimated orders (see text, solid line, bin = 1) of all SS trains was fitted [correlation coefficient (CC) = 0.98] with a gamma process whose order parameter was 3.4 and rate parameter was 0.9 (dotted line).

PCs passively integrate strong excitatory inputs composed of numerous small PF inputs, which are not balanced by inhibitory inputs (Softky & Koch, 1993). Several conditions must be fulfilled for this

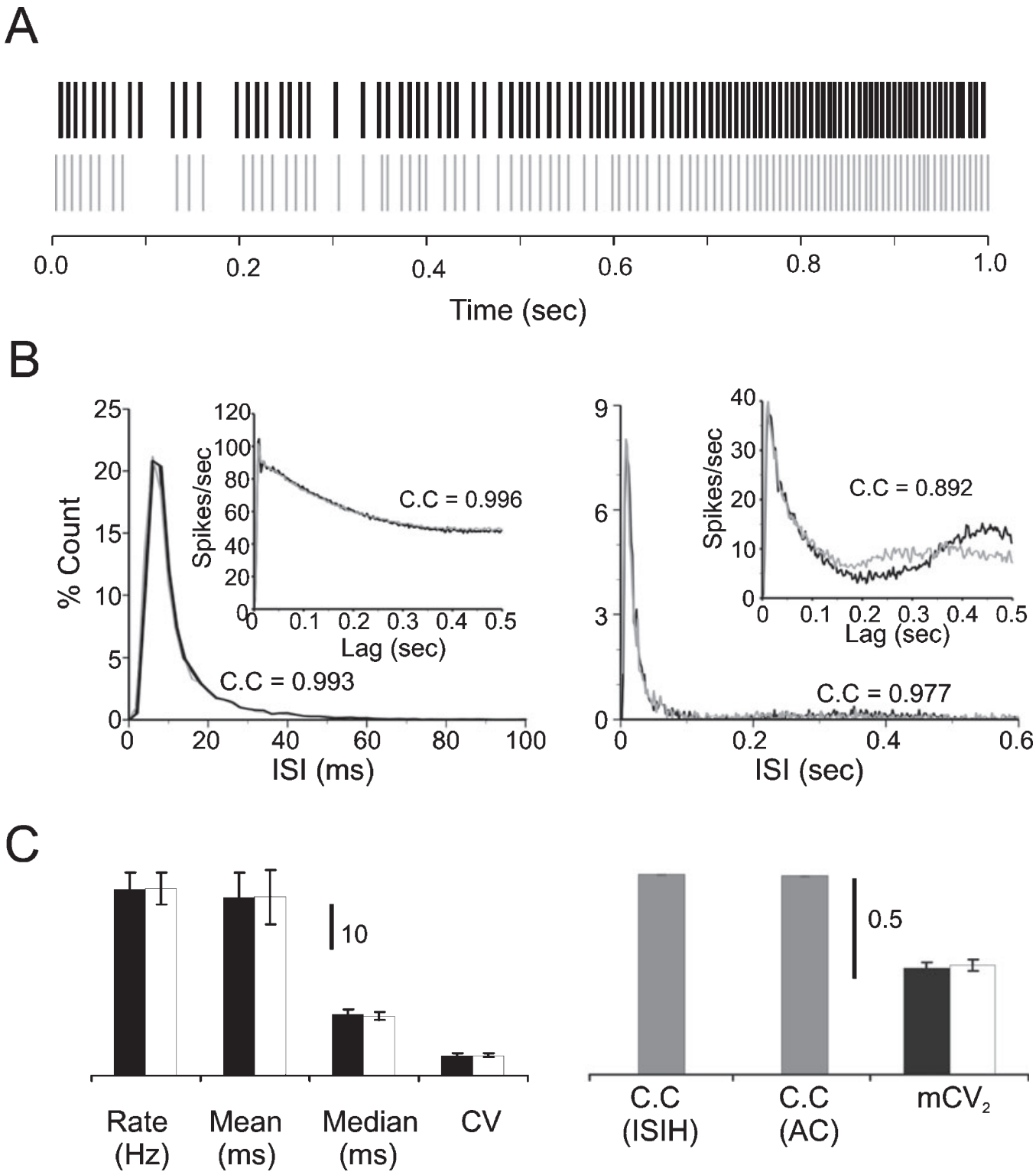

FIG. 11. Statistical properties of simulated simple spike (SS). (A) Representative raster plots of actual SS firing (black lines) and corresponding simulated SSs (gray lines). (B) Two examples of interspike interval (ISI) distributions and autocorrelograms (insets). (C) Averaged rate, mean, median, coefficient of variation (CV) (right) and correlation coefficients (CCs) of ISI histograms and autocorrelograms, and mean of the CV_2 values (mCV_2) (right) were similar between actual (black filled bars) and simulated (open bars) SS trains ($P > 0.5$).

hypothesis. First, the multiple PF inputs have to be independent, which is likely because each PF comes from a different granule cell. Second, unitary excitatory postsynaptic potentials (EPSPs) should be small enough to necessitate the summation of many EPSPs to reach spiking threshold. If all PF inputs are independent and if PCs simply integrate EPSPs to reach threshold, which may be about 10 mV from the resting state (Isope & Barbour, 2002), the number of EPSPs required to make PC firing regular represents the order of the gamma

function (Tuckwell, 1989). Our approximated mean order of regular patterns (110) would thus require unitary EPSPs to be about 0.09 mV, which is indeed in the range of reported values of 0.07 ± 0.06 mV (Isope & Barbour, 2002). However, the spontaneous activity of granule cells *in vivo* has been reported to be of very low rate (0.5 ± 0.2 Hz) (Chadderton *et al.*, 2004). This raises the question of how enough PF activity could be provided to maintain the long regular patterns that we observed in spontaneous SS trains (Shin *et al.*, 2004). An alternative explanation could be that regular patterns are due to intrinsic firing of PCs (Loewenstein *et al.*, 2005), whereas PF inputs are only important for triggering them and for controlling the order of the regular patterns, e.g. by controlling the firing threshold or, rather, the distance to threshold.

The next question is how singles are generated. It has been reported that the synapses made by the ascending axon of granule cells may be stronger than PF synapses (Gundappa-Sulur *et al.*, 1999; Isope & Barbour, 2002; Grillner *et al.*, 2005). By the argument given above, larger EPSPs will lower the order of the gamma function (Tuckwell, 1989). Thus, the 20 times lower order of singles is explained if singles are caused by the ascending input only. A more likely explanation, however, is that they are caused by the feed-forward inhibition pathway through molecular layer interneurones considering the longer ISIs (Fig. 10A) of singles. Activation of the neurones that inhibit PCs with a latency of 1 ms (Mittmann *et al.*, 2005) will cut short the regular patterns, hyperpolarize the membrane potential and cause the next ISI to be longer. We recently reported that pauses in SS firing, which consist mostly of singles, are synchronized among nearby PCs (Shin & De Schutter, 2006), a finding that is also most easily explained by inhibition from common molecular layer interneurones. This viewpoint is also supported by the observation that PCs become more regular if molecular layer interneurones are blocked (Hausser & Clark, 1997). Another potential source of singles with very long ISIs is the down states of bistable PCs (Loewenstein *et al.*, 2005).

Taken together, these findings indicate that both the very irregular CS and SS firings can be described with a mixture of gamma processes. Although this stochastic simplification of PC firing does not explain the underlying mechanisms *per se*, it will be a useful constraint for more mechanistically orientated explanatory models of PC spiking *in vivo*.

Acknowledgements

This work was supported by grants from the Inter-University Attraction Pole, Medical Foundation Queen Elizabeth, Fonds Wetenschappelijk Onderzoeck, and Bundesministerium für Bildung und Forschung.

Abbreviations

CS, complex spike; CV, coefficient of variation; EPSP, excitatory postsynaptic potential; ISI, interspike interval; mCV_2, mean of the CV_2 values; PC, Purkinje cell; PF, parallel fibre; SS, simple spike.

References

Bower, J.M. & Woolston, D.C. (1983) Congruence of spatial organization of tactile projections to granule cell and Purkinje cell layers of cerebellar hemispheres of the albino rat: vertical organization of cerebellar cortex. *J. Neurophysiol.*, **49**, 745–766.

Brown, I.E. & Bower, J.M. (2001) Congruence of mossy fiber and climbing fiber tactile projections in the lateral hemispheres of the rat cerebellum. *J. Comp. Neurol.*, **429**, 59–70.

Chadderton, P., Margrie, T.W. & Hausser, M. (2004) Integration of quanta in cerebellar granule cells during sensory processing. *Nature*, **428**, 856–860.

Dayan, P. & Abbott, L.F. (2001) *Theoretical Neuroscience: Computational and Mathematical Modeling of Neural Systems*. MIT Press, Cambridge, MA.

Ebner, T.J. & Bloedel, J.R. (1981) Temporal patterning in simple spike discharge of Purkinje cells and its relationship to climbing fiber activity. *J. Neurophysiol.*, **45**, 933–947.

Gabbiani, F. & Koch, C. (1998) Principles of spike train analysis. In Koch, C. & Segev, I. (Eds), *Methods in Neural Modeling.* MIT Press, Cambridge, MA. pp. 313–360.

Goossens, J., Daniel, H., Rancillac, A., van der Steen, J., Oberdick, J., Crepel, F., De Zeeuw, C.I. & Frens, M.A. (2001) Expression of protein kinase C inhibitor blocks cerebellar long-term depression without affecting Purkinje cell excitability in alert mice. *J. Neurosci.*, **21**, 5813.

Grillner, S., Markram, H., De Schutter, E., Silberberg, G. & LeBeau, F.E. (2005) Microcircuits in action − from CPGs to neocortex. *Trends Neurosci.*, **28**, 525–533.

Gundappa-Sulur, G., De Schutter, E. & Bower, J.M. (1999) Ascending granule cell axon: an important component of cerebellar cortical circuitry. *J. Comp. Neurol.*, **408**, 580–596.

Hausser, M. & Clark, B.A. (1997) Tonic synaptic inhibition modulates neuronal output pattern and spatiotemporal synaptic integration. *Neuron*, **19**, 665–678.

Holt, G.R., Softky, W.R., Koch, C. & Douglas, R.J. (1996) Comparison of discharge variability in vitro and in vivo in cat visual cortex neurons. *J. Neurophysiol.*, **75**, 1806–1814.

Isope, P. & Barbour, B. (2002) Properties of unitary granule cell –> Purkinje cell synapses in adult rat cerebellar slices. *J. Neurosci.*, **22**, 9668–9678.

Keating, J.G. & Thach, W.T. (1995) Nonclock behavior of inferior olivary neurons: interspike intervals of Purkinje cell complex spike discharge in the awake behaving monkey is random. *J. Neurophysiol.*, **73**, 1329–1340.

Lang, E.J., Sugihara, I., Welsh, J.P. & Llinas, R. (1999) Patterns of spontaneous purkinje cell complex spike activity in the awake rat. *J. Neurosci.*, **19**, 2728–2739.

Llinas, R. & Yarom, Y. (1986) Oscillatory properties of guinea-pig inferior olivary neurones and their pharmacological modulation: an in vitro study. *J. Physiol. Lond.*, **376**, 163–182.

Loewenstein, Y., Mahon, S., Chadderton, P., Kitamura, K., Sompolinsky, H., Yarom, Y. & Hausser, M. (2005) Bistability of cerebellar Purkinje cells modulated by sensory stimulation. *Nat. Neurosci.*, **8**, 202–211.

Manor, Y., Rinzel, J., Segev, I. & Yarom, Y. (1997) Low-amplitude oscillations in the inferior olive: a model based on electrical coupling of neurons with heterogeneous channel densities. *J. Neurophysiol.*, **77**, 2736–2757.

Mittmann, W., Koch, U. & Hausser, M. (2005) Feed-forward inhibition shapes the spike output of cerebellar Purkinje cells. *J. Physiol.*, **563**, 369–378.

Nawrot, M.P., Aertsen, A. & Rotter, S. (2003) Elimination of response latency variability in neuronal spike trains. *Biol. Cybern.*, **88**, 321–334.

Sato, Y., Miura, A., Fushiki, H. & Kawasaki, T. (1992) Short-term modulation of cerebellar Purkinje cell activity after spontaneous climbing fiber input. *J. Neurophysiol.*, **68**, 2051–2062.

Shin, S.L. & De Schutter, E. (2006) Dynamic synchronization of Purkinje cell simple spikes. *J. Neurophysiol.*, **96**, 3485–3491.

Shin, S.L., Aertsen, A. & De Schutter, E. (2004) Hidden temporal structure in Purkinje cell simple spike trains. *Soc. Neurosci. Abstr.* 827.11.

Softky, W.R. & Koch, C. (1993) The highly irregular firing of cortical cells is inconsistent with temporal integration of random EPSPs. *J. Neurosci.*, **13**, 334–350.

Tuckwell, H.C. (1988) Introduction to theoretical neurobiology II. *Nonlinear and Stochastic Theories*. Cambridge University Press, New York.

Tuckwell, H.C. (1989) *Stochastic Processes in the Neurosciences*. Society for Industrial and Applied Mathematics, Philadelphia.

Vos, B.P., Volny-Luraghi, A. & De Schutter, E. (1999) Cerebellar Golgi cells in the rat: receptive fields and timing of responses to facial stimulation. *Eur. J. Neurosci.*, **11**, 2621–2634.

Yarom, Y. & Cohen, D. (2002) The olivocerebellar system as a generator of temporal patterns. *Ann. N.Y. Acad. Sci.*, **978**, 122–134.